Comparison of polar ozone loss rates simulated by one-dimensional and three-dimensional models with Match observations in recent Antarctic and Arctic winters

Om Prakash Tripathi, Sophie Godin-Beekmann, Franck Lefèvre, Andrea Pazmino, Alain Hauchecorne, Martyn Chipperfield, Wuhu Feng, Genevieve Millard, Markus Rex, Martin Streibel, et al.

Comparison of polar ozone loss rates simulated by one-dimensional and three-dimensional models with Match observations in recent Antarctic and Arctic winters

Om Prakash Tripathi,[1,2] Sophie Godin-Beekmann,[1] Franck Lefèvre,[1] Andrea Pazmiño,[1] Alain Hauchecorne,[1] Martyn Chipperfield,[3] Wuhu Feng,[3] Genevieve Millard,[4] Markus Rex,[5] Martin Streibel,[5] and Peter von der Gathen[5]

Received 20 December 2006; revised 6 March 2007; accepted 14 March 2007; published 26 June 2007.

[1] Simulations of ozone loss rates using a three-dimensional chemical transport model and a box model during recent Antarctic and Arctic winters are compared with experimental loss rates. The study focused on the Antarctic winter 2003, during which the first Antarctic Match campaign was organized, and on Arctic winters 1999/2000, 2002/2003. The maximum ozone loss rates retrieved by the Match technique for the winters and levels studied reached 6 ppbv/sunlit hour and both types of simulations could generally reproduce the observations at 2-sigma error bar level. In some cases, for example, for the Arctic winter 2002/2003 at 475 K level, an excellent agreement within 1-sigma standard deviation level was obtained. An overestimation was also found with the box model simulation at some isentropic levels for the Antarctic winter and the Arctic winter 1999/2000, indicating an overestimation of chlorine activation in the model. Loss rates in the Antarctic show signs of saturation in September, which have to be considered in the comparison. Sensitivity tests were performed with the box model in order to assess the impact of kinetic parameters of the ClO-Cl_2O_2 catalytic cycle and total bromine content on the ozone loss rate. These tests resulted in a maximum change in ozone loss rates of 1.2 ppbv/sunlit hour, generally in high solar zenith angle conditions. In some cases, a better agreement was achieved with fastest photolysis of Cl_2O_2 and additional source of total inorganic bromine but at the expense of overestimation of smaller ozone loss rates derived later in the winter.

Citation: Tripathi, O. P., et al. (2007), Comparison of polar ozone loss rates simulated by one-dimensional and three-dimensional models with Match observations in recent Antarctic and Arctic winters, *J. Geophys. Res.*, *112*, D12307, doi:10.1029/2006JD008370.

1. Introduction

[2] Stratospheric ozone depletion and the springtime ozone hole over Antarctica are well-known phenomena, which have been simulated in various modeling studies [e.g., *World Meteorological Organization* (*WMO*), 2003]. In the Antarctic, models have shown their ability to simulate the overall chemical ozone loss, but there have been very few attempts to precisely quantify ozone loss rates in the course of the winter and spring seasons. The estimation of the chemical ozone depletion rate is a key for a proper understanding of ozone loss processes in the polar regions. Most studies on chemical ozone loss rates have concentrated on the Arctic because of the high interannual variability of the Arctic ozone loss in relation with the year-to-year meteorological conditions and the difficulty to diagnose the contributions from dynamical processes and chemical depletion. To isolate chemical ozone change from the dynamical effects, various methods have been proposed, for example, the computation of the chemical loss from observed values of halogen oxides [*Salawitch et al.*, 1990, 1993; *Brune et al.*, 1991], the tracer correlation technique [*Fahey et al.*, 1990; *Proffitt et al.*, 1990, 1993; *Müller et al.*, 1997], or the use of a passive ozone tracer from three-dimensional chemical transport to correct ozone change from observations [*Hansen et al.*, 1997; *Goutail et al.*, 1999, *Goutail et al.*, 2005].

[3] The present study focuses on the Match technique, a Lagrangian approach based on coordinated ozone sondes measurements and trajectory calculations for the estimation of ozone loss within the polar vortex. In this method, the air parcel along a trajectory is probed twice by ozone sonde measurements and the difference between both measure-

[1]Service d'Aéronomie–IPSL du CNRS, Université Pierre et Marie Curie, Paris, France.
[2]Now at NASA–Jet Propulsion Laboratory, California Institute of Technology, Table Mountain Facility, Wrightwood, California, USA.
[3]Institute for Atmospheric Science, University of Leeds, Leeds, United Kingdom.
[4]Department of Earth Sciences, University of Cambridge, Cambridge, United Kingdom.
[5]Alfred Wegener Institute for Polar and Marine Research, Potsdam, Germany.

0148-0227/07/2006JD008370

ments is considered as a chemical ozone change. Chemical ozone loss rates are then determined from the statistical analysis of hundreds of coordinated ozone sonde measurements performed during the winter [*von der Gathen et al.*, 1995; *Rex et al.*, 1997, 1999, 2002]. In the Match technique, care is needed to avoid air masses that experienced large distortion during transport, which often causes mixing. *Grooβ and Müller* [2003] showed that filter criteria involved in the Match technique effectively remove any effect from mixing on the measured ozone loss rates.

[4] The studies on Arctic chemical ozone loss have revealed differences between observations and model simulations with most of the cases' underestimation of ozone loss by the models [e.g., *Becker et al.*, 1998; *Becker et al.*, 2000; *Woyke et al.*, 1999, *Kilbane-Dawe et al.*, 2001]. Most of these studies compared ozone loss rates from ozonesondes and other observations with the loss rate calculated from photochemical box models. The discrepancies between the models and observations generally occur at higher levels during January when the air parcels are exposed to solar radiation at high solar zenith angles [*Rex et al.*, 2003]. Using a bivariate linear regression analysis on the ozone measurements along trajectories, *Rex et al.* [2003] have shown that the ozone loss occurs during sunlight periods only, which rules out the possibility of direct ozone loss on the surface of polar stratospheric clouds during nighttime. The photolysis of the dimer of chlorine monoxide, Cl_2O_2, is fundamentally responsible for the most destructive chlorine-catalyzed ozone loss mechanism [*Molina and Molina*, 1987; *Anderson et al.*, 1991; *Solomon*, 1999]. High solar zenith angles during January limits the availability of UV radiation for photolysis because of long attenuation path and hence reduces the ozone loss in most photochemical box models. The idea of the photolysis of Cl_2O_2 by IR radiation near 800 nm during twilight conditions, which might increase the abundance of Cl in January and consequently enhance the overall ozone loss [*Avallone and Toohey*, 2001; *Vomel et al.*, 2001], was found to be in disagreement with the first coincident measurements of ClO and Cl_2O_2 performed by *Stimpfle et al.* [2004] during the Arctic winter 1999/2000. These measurements indicate, however, a stronger photolysis of Cl_2O_2 in the near UV (300–360 nm) than recommended by JPL-2002 [*Sander et al.*, 2003], and the authors suggested the use of Cl_2O_2 absorption cross-sections from the work of *Burkholder et al.* [1990]. More recently, several studies have focused on the understanding of the kinetics of the ClO-dimer cycle [e.g., *von Hobe et al.*, 2005, 2006]. In the work of *von Hobe et al.* [2006], they suggest a stronger Cl_2O_2 photolysis rate but intermediate between the JPL-2002 assessment and the results of *Burkholder et al.* [1990]. *Vogel et al.* [2006] have studied the role of radical-molecule complexes on polar stratospheric ozone loss processes using the Chemical Lagrangian Model of the Stratosphere (CLaMS). They showed that the existence of ClO_x radical-molecule complexes could possibly explain some discrepancies between laboratory and stratospheric measurements although the potential impact of ClO_x radical-molecule complexes on polar stratospheric ozone loss processes is very small considering pure gas-phases. Other studies have concentrated on the amount of active bromine to be accounted for in lower stratosphere [e.g., *Salawitch et al.*, 2005], suggesting increased levels of inorganic bromine in that region due to short-lived biogenic compounds transported to the stratosphere. All these studies point to a stronger ozone loss due to both the ClO-dimer and ClO–BrO catalytic cycles in the polar regions.

[5] The discrepancies between modeled and observed ozone loss rates particularly in Arctic winters during January have indicated that our quantitative understanding of polar ozone loss may still be incomplete. To address this issue, a coordinated theoretical and experimental study of polar ozone loss was launched under the framework of the European project QUOBI (Quantitative Understanding of Polar Ozone Loss by Bipolar Investigation). For the first time, a Match campaign was launched in Antarctica in the year 2003, and state of the art three-dimensional chemical transport models and one-dimensional photochemical box models were used to simulate ozone loss rates in this region. The project also included a Match campaign in the Arctic in the winter 2002/2003. The various models involved in the project were used to simulate ozone loss rates that occurred this winter and also during other Arctic winters.

[6] The objective of this paper is to assess the capacity of two models involved in the QUOBI project, to reproduce the ozone loss rates deduced from the Match campaigns, and to evaluate the new results regarding ClO kinetic parameters and bromine levels on the simulated loss rates. For this study, we used the high-resolution three-dimensional chemical transport model MIMOSA-CHIM (Modele Isentropique de Transport Méso-échelle de l'Ozone Stratosphérique par Advection avec Chimie) and the REPROBUS (Reactive Processes Ruling the Ozone Budget in the Stratosphere) photochemical box model to simulate the ozone loss rates calculated from the Match technique. The paper is organized as follows: First, we present a short introduction to the models and a description of the technique adopted to obtain from the model outputs ozone matches similar to the experimental ones. Then the main part of the paper is devoted to the comparison of experimental and simulated ozone loss rates for the Antarctic and Arctic winters considered in the study. In a following section, the results of the comparisons are discussed and sensitivity studies on active chlorine and bromine levels in the one-dimensional simulation, on the basis of the latest measurements in recent campaigns, are presented. Finally we summarize the main results and present the conclusions of the work.

2. Models Description

[7] Both Lagrangian and Eulerian type models have been used in the past to compare with Match loss rates. Here the three-dimensional chemical transport model MIMOSA-CHIM and the REPROBUS photochemical box model along Match trajectories are used. This box model uses the chemical module of the three-dimensional CTM REPROBUS [*Lefèvre et al.*, 1994]. In order to better compare the Lagrangian model results, it was decided within QUOBI that the initial chemical fields for the various photochemical box simulations would be provided by one model only, the three-dimensional CTM SLIMCAT. However, three-dimensional simulations within QUOBI could use their own choice of initialization fields. A brief description of all three models involved in this study is provided here.

2.1. Three-Dimensional Chemical Transport Model

[8] The three-dimensional CTM MIMOSA-CHIM is the combination of the dynamical model MIMOSA and the chemistry scheme of three-dimensional CTM REPROBUS [*Lefèvre et al.*, 1998; *Marchand et al.*, 2003; *Tripathi et al.*, 2006]. MIMOSA is initially a potential vorticity (PV) advection model designed for the study of polar filaments [*Hauchecorne et al.*, 2002]. The MIMOSA-CHIM model was developed in order to provide high-resolution ($1^\circ \times 1^\circ$) simulations of the stratospheric polar ozone loss on isentropic levels. The model runs on 16 isentropic surfaces between 350 and 950 K, which results in a vertical resolution of less than 2 km. It starts on a $1^\circ \times 1^\circ$ high-resolution orthogonal grid in an azimuthal equidistant projection centered on the pole. The principle of the model is as follows: Each grid point is advected using meteorological winds from European Centre for Medium-Range Weather Forecasts (ECMWF) operational analyses interpolated on the MIMOSA grid at the specified isentropic level. As the time passes, the orthogonal MIMOSA grid is stretched and deformed by horizontal gradients in the wind field. After a given time (6 hours), the PV and chemical fields are reinterpolated onto the original grid in order to keep the distance between two adjacent points approximately constant. The regridding process produces numerical diffusion, and to minimize this diffusion, an interpolation scheme, based on the preservation of second order momentum of PV perturbation, has been implemented [*Hauchecorne et al.*, 2002]. The chemical fields are initialized using output from the three-dimensional CTM REPROBUS interpolated to the MIMOSA-CHIM grid. The diabatic transport of air across isentropic surfaces is computed from the heating rates calculated using the radiation scheme of the SLIMCAT model taken from MIDRAD [*Chipperfield*, 1999]. Climatological water vapor and CO_2 fields and interactive ozone fields taken from the model itself are used for the calculation of heating rates. The REPROBUS chemical module includes 55 chemical species and calculates about 160 reactions including gas phase, heterogeneous, and photolytic reactions. Photodissociation frequencies are calculated using a four-dimensional lookup table expressed as a function of altitude, solar zenith angle, ozone column, and albedo [*Lefèvre et al.*, 1994]. Cross sections are taken from JPL-2002 photochemical data except for Cl_2O_2 absorption cross sections, which are taken from the work of *Burkholder et al.* [1990], with log linear extrapolation to longer wavelengths as described in the work of *Stimpfle et al.* [2004]. Chlorine species in the REPROBUS chemistry scheme were scaled to reach a total chlorine loading of 3.6 ppbv above 30 km [*WMO*, 1992]. Total bromine in MIMOSA-CHIM is based on a correlation with CFC-11 [*Wamsley et al.*, 1998]. This correlation considers the supply of bromine from CH_3Br, halons, CH_2Br_2, and CH_2BrCl. The model has a scheme of PSC formation and growth through the representation of heterogeneous chemistry as described in the work of *Tripathi et al.* [2006]. Water vapor is one of the constituents included in the chemistry module and is initialized in the three-dimensional CTM REPROBUS simulation from a Microwave Limb Sounder (MLS) climatology. Equilibrium composition and volume of binary (H_2SO_4-H_2O) and ternary (HNO_3-H_2SO_4-H_2O) droplets are calculated using an analytic expression by *Carslaw et al.* [1995]. Liquid supercooled sulphuric acid aerosols, NAT, and ice particles are considered in equilibrium with the gas-phase [*Lefèvre et al.*, 1998]. For NAT and ice particles, the number density is set to 5×10^{-3} cm^{-3}, and the diameter is calculated within the scheme from available volume of HNO_3 and water. Denitrification is introduced through the sedimentation of NAT and ice particles.

2.2. Photochemical Box Model

[9] The REPROBUS chemical scheme has also been used as a box model to calculate the evolution of chemical species along the air mass trajectories computed for the Match campaigns. Since SLIMCAT simulations provide the initial fields for the chemical constituents, some of the chemical parameters in the REPROBUS box model are treated differently than in the MIMOSA-CHIM model. In the REPROBUS box model, total chlorine (Cl_y), Br_y, ClO_x, and BrO are provided by SLIMCAT output fields, while in MIMOSA-CHIM, Cl_y and Br_y sources are different. Box model REPROBUS runs along the trajectories provided by the Alfred Wegener Institut (AWI) Match team, and the maximum length of trajectories are about 10 days. Therefore unlike for MIMOSA-CHIM, there is no separate denitrification scheme for the REPROBUS box model for this short duration, but the long-term seasonal denitrification is taken into account in the chemical fields provided by SLIMCAT for the initialization. The trajectories are calculated by taking into account the diabatic descent. For this, the heating rates for the adjustment of trajectories are calculated using the MIDRAD scheme [*Shine*, 1987].

2.3. Initial Fields From SLIMCAT Three-Dimensional Chemical Transport Model

[10] The SLIMCAT three-dimensional off-line CTM was used within QUOBI to provide initial fields for the photochemical box model simulations (for detailed information on SLIMCAT, see the works of *Chipperfield* [1999] and *Chipperfield et al.* [2005]). In addition to the tropospheric source gases specified in *WMO* [2003] (halocarbons CFC-11, CFC-12, CFC-113, CCl_4, CH_3CCl_3, CH_3Cl, HCFC-22 for chlorine and CH_3Br, $CBrClF_2$, $CBrF_3$, CH_2Br_2, CH_2BrCl for bromine), an extra 100 pptv of chlorine and 6 pptv of bromine is added, making 3.7 ppbv of total chlorine and 21 pptv of total bromine, which are assumed to reach the stratosphere from short-lived halogen source gases [*Feng et al.*, 2005]. SLIMCAT uses photochemical data from JPL-2002 except, as in REPROBUS, for Cl_2O_2 absorption cross-sections, which are taken from the work of *Burkholder et al.* [1990]. SLIMCAT differs from REPROBUS in the way the reaction probability (γ) of the heterogeneous reaction ($ClONO_2$ + $HCl \rightarrow Cl_2 + HNO_3$) is treated. The reaction probability on NAT surface in REPROBUS is constant and does not depend on temperature so the strong chlorine activation starts early in the winter. In SLIMCAT, the reaction probability is inversely dependent on temperature, and therefore chlorine activation starts later when sufficiently low temperature is achieved. The version of SLIMCAT providing initial fields for this study [*Feng et al.*, 2005; *Chipperfield et al.*, 2005] is formulated using a hybrid σ-θ vertical coordinate. An important change is the introduction of a radiation scheme on the basis of NCAR CCM [*Briegleb*, 1992] instead of the MIDRAD scheme (used in MIMOSA-CHIM) to calculate the heating rates, which improves the modeled transport at

high latitudes. The denitrification due to the sedimentation of PSC particles is simulated using a NAT-based denitrification scheme described by *Davies et al.* [2002]. Use of NAT-based denitrification code (where a portion of the large aerosols was assumed to be NAT instead of just ice) increases available ClO_x but not Cl_y later in the winter.

3. Match Simulation

3.1. Match Technique

[11] The determination of the chemical ozone loss from the Match technique is based on the statistical analysis of ozone loss from various Match events. A Match event is defined as the probing of the same air mass twice at different locations and time. The accumulated ozone loss during a particular time range in an air mass depends on the time interval during which the air mass is exposed to the solar radiation (sunlit hours) and also on the solar zenith angle during that period. Since the variation due to solar zenith angle is already accounted for in the calculation of J (rate of photodissociation) values, ozone loss rates are calculated using total sunlit hours, and variations of solar zenith angle along the trajectory are ignored. Ozone loss rates are calculated using the match events provided by the Match team, according to the method described in *Rex et al.* [2002]. To calculate the ozone loss rate during a particular period, a linear regression is performed between the ozone change within each Match event that occurred during that period and the total sunlit hours. The slope of the regression line gives the ozone loss rate in volume parts per billion per sunlit hours during the period in consideration. Because the ozone loss should be zero for zero sunlit hours, the regression line is forced to pass through the origin [*Rex et al.*, 1999, 2002]. A recent error analysis performed for Match results by *Lehmann et al.* [2005] shows that in order to account for the autocorrelation between the various soundings, the usual standard deviation error should be increased by about 15%. In this study, the error calculated by the regression has thus been increased by 15% in all results. The 2-σ modified error bars, also called 2-σ uncertainty hereafter, are shown in all results described in this paper.

3.2. Match From Three-Dimensional CTM MIMOSA-CHIM

[12] The model starts from the beginning of the winter and runs through the spring period. Start and end dates are 1 June to 30 November for the Antarctic and 1 November to 30 April for the Arctic except in 1999–2000 when constraints of initial data availability made us start the run from 13 December to 30 April. For Match events from the MIMOSA-CHIM three-dimensional output, we adopted the closest approach method. In this method, we capture the events in the model by approaching the event spatially and temporally as close as possible within the limit of the resolution of the model. The coordinate of the location of each sonde measurements, including complete temporal and spatial information, is fed into MIMOSA-CHIM runs. During the simulation, the closest point of each ozonesonde measurements is reached, and the corresponding value of ozone and other compounds is recorded. The time resolution of the advection process of the model is 1 hour, but the chemical scheme runs four times in an hour, so for the concentration of the chemical species, the results are available every 15 min. In that way, the maximum time difference between the measurement and model results cannot exceed 7 min. After temporally approaching the event, the closest isentropic level is determined, and the distance between the location of the measurement and each grid point of that level is computed. The grid point that is closest to the observation is considered for the record. The value of desired chemical compounds at this point is then linearly interpolated to the isentropic level of the measurement. Match events are generally determined at the 425, 450, 475, or 500 K levels. Since the model was run at 16 isentropic levels between 350 and 950 K, the interpolation along the isentropic coordinate is limited to a maximum of 10 K, which is a good approximation. At the time of capturing the ozone value, the model grid may be deformed, but as MIMOSA-CHIM is a high-resolution model regularly regridded, the distance between adjacent grid points does not increase beyond a maximum of 20%, and the measurements can be reached within a range of 0.6° in latitude and longitude. At the end of the run, we have a model event corresponding to each Match event.

[13] Passive ozone tracers were also transported alongwith PV within MIMOSA-CHIM in order to take into account ozone loss due to transport effect within the model between both Match points. In order to limit the divergence between the passive and reactive ozone, 10-day interval tracers were introduced in the calculation. The 10-day tracers were initialized at an interval of 10 days with the current value of reactive ozone at that moment. All the tracers once initialized were advected along PV throughout the course of the simulation. The ozone tracer value corresponding to the first point of a Match event was taken from the latest initialized tracer, and the same transported tracer was used for the second point. So for each Match event, the passive ozone tracer was not older than 10 days. In a perfectly isolated trajectory, the ozone tracer should not change between two points of a Match event. But as described above, because of the resolution limit of the three-dimensional model, the starting and ending points may differ by a maximum of 0.6° in latitude and longitude with the actual Match pairs. Because of the high resolution of the model and the nature of winter polar circulation, it is a good approximation to consider that the modeled starting and ending points belongs to the same air mass if not to the same trajectory. In order to account for possible transport effect linked to the advection and regridding schemes of the model between both points of each simulated Match event, the difference in ozone tracer is taken into account in the computation of ozone loss rates. The corrected ozone difference representing the model chemical ozone loss in a Match event is thus computed using the following formula

$$\Delta OZ_{corr} = (OZ_2 - OZ_1) - (TRA_2 - TRA_1) \quad (1)$$

This corrected ozone difference is regressed with total sunlit hours provided by the AWI Match team in order to evaluate the modeled chemical ozone loss rate. For comparison, the raw ozone loss rate, which includes chemistry as well as

transport within the model, is calculated by regressing the ozone difference ($OZ_2 - OZ_1$) against the total sunlit hours.

3.3. Match From REPROBUS Box Model

[14] For the quantitative comparison of Match results with the REPROBUS box model, we simulated the ozone chemistry along each Match trajectory provided by AWI. The trajectories are calculated from the position of the first ozone sonde measurement of a Match event using ECMWF data. The diabatic evolution of the air masses is taken into account in calculating the trajectories by the diabatic cooling/heating rates provided by the MIDRAD radiation scheme. Each trajectory starts 9–10 days ahead of the first sonde launch and extends 11 days beyond the first measurement. The box model starts at the beginning of the trajectory and goes till the end. In between, it captures the ozone value at the location of the first and second measurements. The chemical species for the initialization of the model at the start of the trajectory were used from the output of latest version of SLIMCAT described above [*Chipperfield et al.*, 2005; *Feng et al.*, 2005]. The evaluation of the ozone loss rate for the box model analysis is similar to that of the three-dimensional MIMOSA-CHIM model Match analysis described above with the exception that no tracer correction is included because of the formulation of the model.

4. Comparison of Results

[15] Our main focus of discussion is the comparison of experimental and modeled ozone loss rates during the Antarctic winter 2003 and Arctic winters 1999/2000 and 2002/2003. For each winter, we compared the experimental loss rates with REPROBUS box model and with three-dimensional MIMOSA-CHIM simulations. Along with ozone loss rates, total reactive chlorine (ClO_x = ClO + $2Cl_2O_2$) and total reactive bromine (BrO_x = BrO + BrCl) are shown at the top of each panel. ClO_x and BrO_x are involved in the two most efficient catalytic cycles responsible for the ozone destruction in the polar regions [*WMO*, 2003]. The plots display the mean initialized values of ClO_x and BrO_x at the first point of the set of Match trajectories considered for the calculation during each period, and the error bars denote 2-σ standard error. In the case of the REPROBUS box model, the ClO_x and BrO_x values were directly provided by SLIMCAT.

4.1. Antarctic Winter 2003

[16] The Antarctic stratosphere during winter/spring provides excellent conditions to test the contemporary heterogeneous and chemical reactions used in the simulations of polar stratospheric ozone losses. The well-formed and isolated Antarctic winter polar vortex generally inhibits extra-vortex dynamical influence in the calculation of ozone loss rates above about 425 K [e.g., *Godin et al.*, 2001]. Coordinated ozonesondes were launched for the first time ever at various Antarctic stations as part of the QUOBI Match campaign organized in the southern hemisphere, and ozone loss rates at 475 and 500 K isentropic levels are calculated and compared with model results. The comparison of the ozone change rates along the trajectories simulated by the box model and the three-dimensional CTM with the Match analysis is displayed in Figure 1 left and right panels, respectively. In the remaining part of the paper, the ozone change rates will also be referred to as ozone loss rates since they are generally negative in the polar stratosphere in winter; ozone loss rates correspond to the absolute value of the displayed ozone change rates.

[17] In the Figure, the error bars representing 2-σ uncertainty of the linear regression are generally much smaller for the model results, especially the photochemical box model, than the experimental ones. This reflects the larger variability of ozone measurements because of random errors and small-scale variability not represented in the simulations. The results show that the largest ozone loss rates are retrieved in the end of August and beginning of September, with a maximum value for the experimental loss rate of 6 ppbv/sunlit hour at 475 K and 5 ppbv/sunlit hours at 500 K. The experimental loss rates are also characterized by large values of the order of 4–5 ppv/sunlit hours in the beginning of July. This double-peak behavior of the experimental loss rates is not reproduced by the models, which simulate a gradual increase of the ozone loss rates from July to the beginning of September. The maximum observed ozone loss rates are smaller than those derived from the Match technique applied to POAM measurements [*Hoppel et al.*, 2005]. In this study, Hoppel et al. found maximum ozone loss rates of 10 ppbv/sunlit hour at the beginning of September 2003 using ECMWF winds. Yet the different sampling of the vortex by both types of measurements makes it difficult to directly compare the experimental results.

[18] The comparison between the REPROBUS box model simulations and the Match observations displays the same characteristics at both 475 and 500 K levels, with an overestimation of the ozone loss rates by the model in August and an underestimation of the loss rates in September. At 475 K, the simulated loss rates are slightly outside the 2-σ error bars of the Match results. In both cases however, the largest experimental ozone loss rates retrieved in the beginning of September are reached by the simulations, although somewhat shifted in time in the lowermost level.

[19] Ozone loss rates deduced from MIMOSA-CHIM simulations are in general lower than those derived from the box model. This can be related to the lower active chlorine levels (by as much as 1 ppbv at 475 K) simulated by the three-dimensional model. The differences in active chlorine levels between SLIMCAT, which provides the initial fields for the one-dimensional simulation and MIMOSA-CHIM, is primarily due to the different schemes used for the calculation of subsidence [*Chipperfield et al.*, 2005]. Yet the better agreement at 500 K with the MIMOSA-CHIM model from the beginning of August indicates that active chlorine may be overestimated in the box model simulation during that period. Indeed, the simulated active chlorine exceeds 3 ppbv with a maximum amount of ClO of 2.35 ppbv along the trajectories. Recently published ClO measurements by MLS on board AURA showed maximum values of 2 ppbv at 490 K between 70° and 75° of equivalent latitude during the 2004 Antarctic ozone hole [*Santee et al.*, 2005]. Maximum mixing ratios of 2 ppbv were also measured by the SMR instrument on board ODIN [*Ricaud et al.*, 2005] and the MIPAS instrument on board ENVISAT [*Glatthor et al.*, 2004] prior to the major warming in 2002. Both studies stated that the vortex was fully activated before the major warming. All these measurements tend to indicate that the amount of ClO

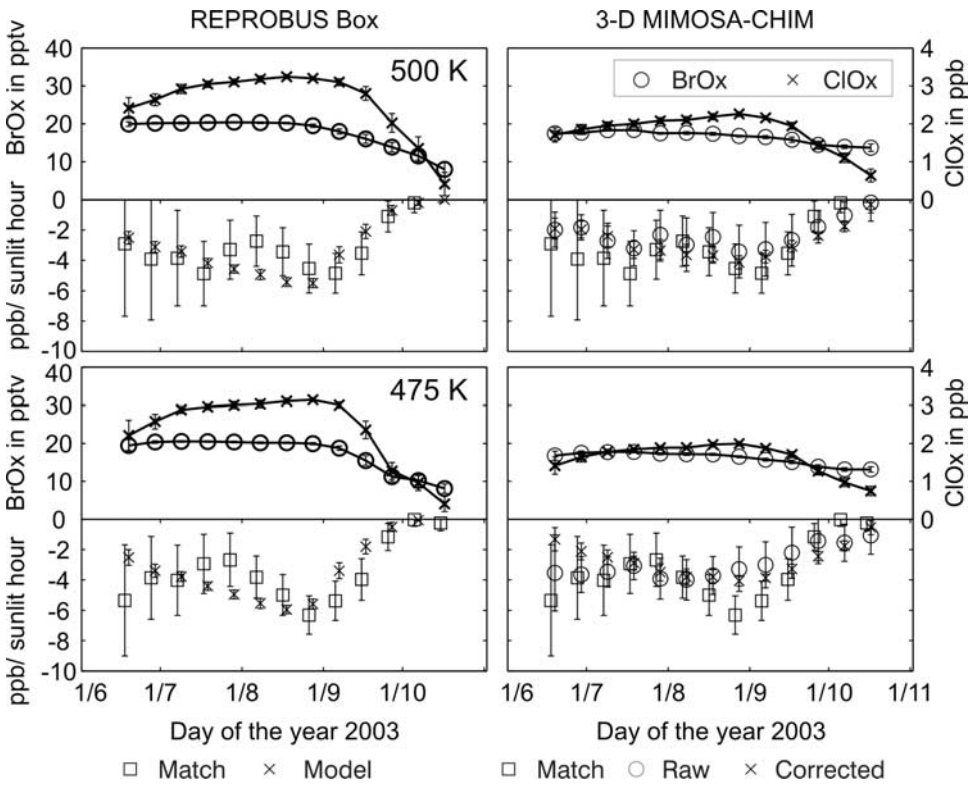

Figure 1. First column shows ozone loss rates in volume parts per billion per sunlit hour at 500 and 475 K deduced from REPROBUS box model simulation compared with Match results (squares) along with the mean initialized ClO_x and BrO_x (top panel) corresponding to each set of Match trajectories for the Antarctic winter 2003. Error bars in ozone loss rates denote 2-σ uncertainty in the linear regression. In ClO_x and BrO_x plots, the error bars denote the 2-σ standard error. The second column display raw and corrected ozone loss rates (see text for detail) from three-dimensional MIMOSA-CHIM along with Match results with mean ClO_x and BrO_x at first point of Match. The legend for top panel of each block is same and is shown only in a few of them. The legend for bottom panel of each column is shown at the bottom of the figure.

in the box model simulation may be too high. However, differences in local time, spatial, and vertical sampling together with the vertical resolution and the uncertainty of the measurements (estimated to 15–20%) make it difficult to directly assess modeled ClO with observations.

[20] The overestimation of the loss rates derived from MIMOSA-CHIM at the end of September and beginning of October is due to the larger active halogen levels simulated by the model at that time as compared to the one-dimensional simulation and to the fact that ozone has not been completely destroyed in the simulation by the end of September as it is the case in observations. In fact, the examination of the experimental and simulated ozone values involved in the various Match events used in the regressions reveals signs of saturation of the depletion process already in the beginning of September for the ozone values simulated by the box model. The effect of saturation is indicated by similar very low ozone values in the first and second measurements of a Match event. The saturation affects retrieved ozone loss rates shown in Figure 1 from the regression period centered on day 240 (very end of August) in the case of the box model and from that centered on day 260 (mid-September) in the case of Match observations. In the former case, only two Match events are affected by saturation on day 240, which can be considered as negligible since the regression is based on 109 Match events. Yet, for the regression centered on day 250, about 15% of Match events are saturated. With the three-dimensional simulation, the ozone depletion does not get to saturation before mid-October after the end of the Match campaign and ozone values simulated by MIMOSA-CHIM never reach zero during the period under study. The effect of saturation largely explains the rapid decrease of ozone loss rates in the course of September in the case of the box model simulation and Match observations.

[21] The influence of transport effects within the three-dimensional simulation as shown by the difference between the grey circles and the black crosses is most pronounced at 475 K in the beginning of the winter and also to some extent in August and September. Discrepancies in the very beginning of the period are to be looked at with caution because of the generally smaller number of points involved in the linear regressions that determine the loss rates (for example, 23 points around 15 June as compared with 92 points on 15 September). In late August and September, the difference between the raw and corrected ozone loss rates indicates a small systematic effect of mixing. This is due to inhomogeneities in the modeled ozone fields caused by chemical destruction. There is a visible discrepancy between the raw and corrected loss rates of about 1.1 ppbv/sunlit hour during mid-September. Since the ozone sounding stations

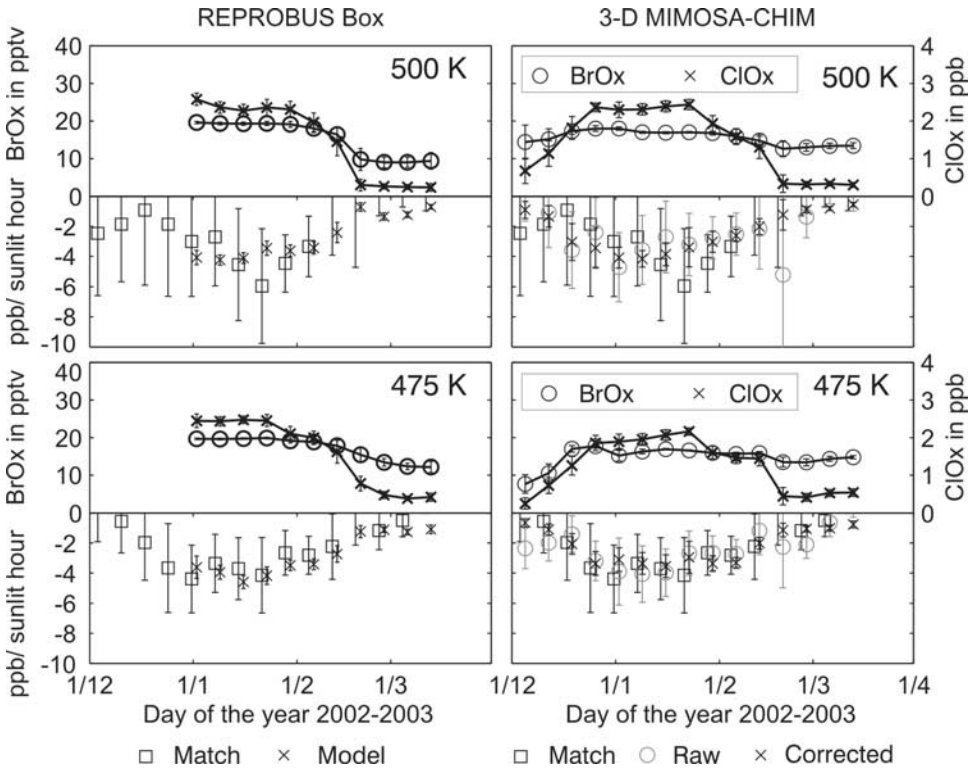

Figure 2. Same as Figure 1 but for the Arctic winter 2002/2003 at 500 and 475 K isentropic levels. Note that Match data are available since December, but REPROBUS box model was run for data since January because of the limitation in SLIMCAT initialization fields.

essentially sample the edge of the polar vortex where ozone destruction is most pronounced, the dynamical processes will tend to flatten ozone gradients and increase ozone levels at the edge of the vortex. This increase is taken into account in the correction, and the corrected ozone loss rates are thus larger than the raw ozone loss rates, which improve the agreement with Match. Such an effect cannot be simulated by the box models which do not simulate mixing processes. This transport effect explains the somewhat better agreement between the three-dimensional simulation and Match observations as compared with the one-dimensional one despite much less active chlorine simulated in the model.

4.2. Recent Arctic Winters

4.2.1. Winter 2002/2003

[22] In the frame of QUOBI, a MATCH campaign was also organized in the Arctic winter 2002/2003 [*Streibel et al.*, 2006]. This winter was characterized by very low temperatures in December which triggered early chlorine activation and consequently early onset of ozone depletion [*Tripathi et al.*, 2006; *Goutail et al.*, 2005]. The ozone loss rates simulated by the one- and three-dimensional models in a similar way as for the Antarctic Match campaign were compared to the experimental Match loss rates at 475 and 500 K. The results are displayed in Figure 2.

[23] The experimental ozone loss rates retrieved during this Arctic winter are, in general, smaller than those retrieved in the Antarctic winter 2003 with maximum values of 4 ppbv/sunlit hours at 475 K. At 500 K, a maximum ozone loss rate of 6 ppbv/sunlit hour was found at the end of January but with rather large error bars. According to the Match experiment, the chemical ozone loss took place up to about mid-February [see also *Streibel et al.*, 2006]. After that period, no ozone loss was found at 500 K, and very small ozone loss rates were computed at 475 K. After the very cold meteorological conditions in early winter, the polar vortex became quite disturbed in January with a major warming in mid-January which split the vortex in the upper stratosphere and a minor warming in February. These disturbances inhibited the formation of PSC and suppressed the conditions for large-scale ozone depletion.

[24] The simulated ozone loss rates show generally a better agreement with the experimental results as compared with the Antarctic simulations, with nearly all the model points lying within the 2-sigma error bars of the Match results, except at the very end of the campaign in March. During that period, both models still simulate some ozone loss rates between 0.5 and 1 ppbv/sunlit hour, while no ozone loss is retrieved by Match. This sustained ozone loss is linked to the remaining active chlorine still present in both simulations during that period. At 500 K, both models underestimate by about 1.5 ppbv/sunlit hour, the maximum ozone loss rates of 6 ppbv/sunlit hour retrieved by Match in the third week of January. Yet model results are within the 2-σ error bars of the experimental values. At that level, the amount of active chlorine simulated by both models is very similar, which explains the rather good agreement between the simulations. At 475 K, excellent agreement is generally found between the modeled and experimental results. The ozone loss rates simulated by MIMOSA-CHIM in January are slightly smaller than those from the box model. This discrepancy can be explained by larger active chlorine and

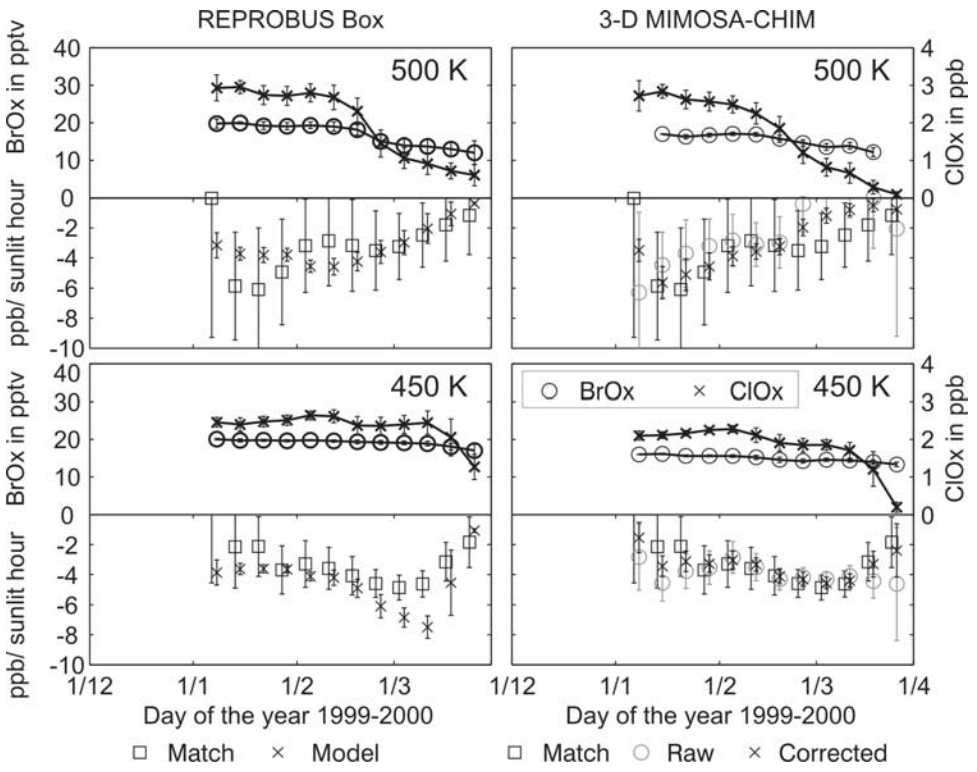

Figure 3. Same as Figure 2 but for the Arctic winter 1999/2000 and at 500 and 450 K isentropic levels.

bromine levels simulated by the box model in January, which amount in average to 2.4 ppbv and 20 pptv, respectively, as compared with 1.8 ppbv and 16 pptv in the one-dimensional simulation. Transport effects are rather small at both levels in the three-dimensional simulation. The large raw ozone loss rate found at 500 K in the second half of February can be related to both the poor statistics of the regression performed on 15 points only and the effect of the minor warming in the model fields. Some transport effects are also seen at 475 K at the beginning and at the end of the campaign. They may indicate some mixing within the model simulation of air masses from outside the vortex and characterized by lower ozone levels. Such systematic transport effects are most visible when the polar vortex is less stable as in the beginning and end of the winter or during major and minor warming events. They are also found in the presence of large ozone gradients as in the Antarctic region, linked to variation of the air subsidence or the chemical destruction within the polar vortex.

4.2.2. Winter 1999/2000

[25] In addition to the analysis of the Match campaigns organized within QUOBI, the Arctic winter 1999/2000 was chosen as a test for the models involved in the project. This winter was among the coldest ones in the last decade, with temperatures in the low stratosphere below the threshold for PSC formation for a large number of days [*Manney and Sabutis*, 2000]. The Match campaign which took place during that winter was organized within the broader THESEO/SOLVE 2000 campaign, the objective of which was to improve the understanding of Arctic ozone loss from a large set of airborne, ground-based, and balloon borne measurements [*Newman et al.*, 2002]. The results of the comparison between the one- and three-dimensional simulations and the Match results in 1999/2000 are shown in Figure 3. They are provided at the 450 and 500 K isentropic levels because of the nonavailability of Match data at 475 K.

[26] As compared to the winter 2002/2003, Match ozone loss rates at 500 K are larger in January with values between 5 and 6 ppbv/sunlit hours in the first 3 weeks of the month. Yet the experimental error bars are also quite large at that level. At 450 K, the largest ozone loss rates are retrieved in February–March, with a maximum of 4.8 ppbv/sunlit hour in the beginning of March. The comparison with the simulations shows more contrasted results as for the 2002/2003 Arctic winter. In the case of the box model, the best agreement is observed at 500 K, with the model points lying within the 2-σ uncertainty of the experimental results throughout the winter. Agreement is achieved because of the large experimental error bars at that level and despite a systematic underestimation of the observed loss rates in January. Reversely, at the lowermost level, the modeled loss rates are systematically larger than the Match ones with a significant disagreement at 2-σ level in the beginning of March. The fact that a much better agreement is obtained at that level with the three-dimensional simulation indicates that the active halogen amounts may be overestimated in the SLIMCAT initialization fields. Indeed, simultaneous measurements of ClO and Cl_2O_2 by *Stimpfle et al.* [2004] on board the ER-2 around 450 K potential temperature level during that winter showed 2 ppbv of ClO_x on 2 February during the day and 1.5 ppbv on 11 March. These values are closer to those simulated by MIMOSA-CHIM than by the box model with SLIMCAT initialization.

[27] In contrast to other winters, ozone loss rates from the three-dimensional simulation show significant effect of

transport throughout the winter at 500 K. While the corrected ozone loss rates are in very good agreement with Match loss rates in January, the raw ozone loss rates are underestimated. Yet the retrieved values are still within the 2-σ error bars of the experimental results. In March, the model fails to reproduce the observations. The raw ozone change rates show an actual increase of ozone while the corrected ones are closer to the Match results. The corrected ozone loss rates still underestimate systematically the experimental results but they are within the 2-σ experimental error bars. Maps of the simulated ozone field in March show large ozone gradients within the vortex because of chemical destruction (not shown), with ozone strongly depleted in the core of the vortex. Transport effects will then tend to increase ozone in that region. Figure 7 in the work of *Rex et al.* [2002], which displays the sampling of the polar vortex with Match events at various levels in the winter 1999/2000, shows that most ozone soundings took place in the core region at that level in March.

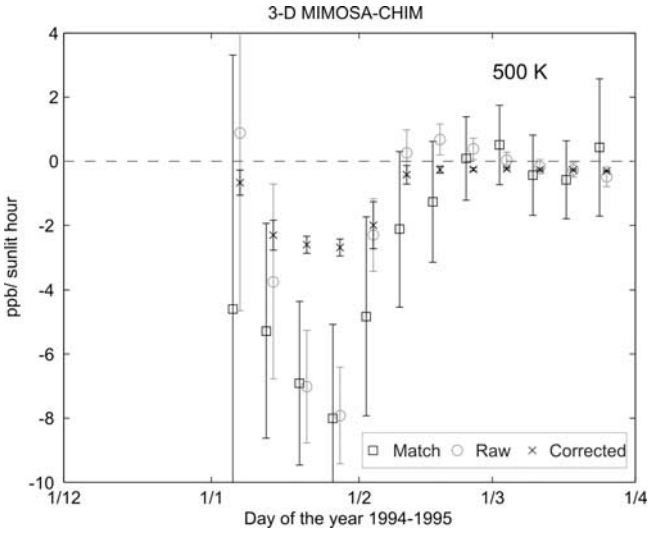

Figure 4. Raw and corrected ozone loss rates from three-dimensional MIMOSA-CHIM along with Match results with 2-sigma uncertainty for Arctic winter 1994–1995 at 500 K.

5. Discussion of Results and Sensitivity Tests

5.1. Transport Effects in the Three-Dimensional Simulation

[28] The model results, when compared with observations, indicate the ability of the tested models to reproduce the analyzed result from the observations. In some cases, excellent agreement is achieved with observed results but some discrepancies still persist. As shown for the three-dimensional MIMOSA-CHIM simulations, transport processes within the model can play a role in these differences. The transport scheme of MIMOSA-CHIM and its ability to represent transport and filamentation processes have already been evaluated in previous works for specific events [*Heese et al.*, 2001; *Godin et al.*, 2002]. To assess the accuracy of MIMOSA-CHIM for Match-type studies and compare the simulations with published results from other three-dimensional models, we calculated ozone loss rates for the Arctic winter 1994/1995 with MIMOSA-CHIM using Match trajectories as described in section 4. Indeed, older SLIMCAT simulations for the winter of 1994/1995 suggested that the Match method may have overestimated the ozone loss rates at higher levels in January 1995 because of a large midlatitude air intrusion and a poor isolation of the trajectories at these levels [*Kilbane-Dawe et al.*, 2001]. The Arctic winter 1994/1995 was among the coldest one and severe ozone loss was observed in January with ozone loss rates approaching 8 ppbv/sunlit hour. No simulation from REPROBUS was available to initialize MIMOSA-CHIM for that winter, and the pressure range of ECMWF meteorological fields was limited to 10 hPa, so we used SLIMCAT [*Chipperfield et al.*, 1996] chemical fields and UKMO (United Kingdom Met Office) meteorological analyses for the wind and temperature data (although the trajectory calculation uses ECMWF analysis). It should be noted here that this test on winter 1994/1995 was made in order to show the possible importance of transport processes in three-dimensional models while calculating Match ozone loss rates. It is assumed here that the trajectories calculated using ECMWF and UKMO winds are, if not identical, close to each other and represents same type of air masses. The results from three-dimensional MIMOSA-CHIM are shown in Figure 4 for the 500 K isentropic level. An excellent agreement is found in the three-dimensional simulation case between the simulated raw ozone loss rates and Match loss rates. However, the corrected loss rates severely underestimate the observed ones, which indicate a systematic effect of transport at that level as described in the work of *Kilbane-Dawe et al.* [2001]. This test shows thus that transport effects have to be evaluated when comparing three-dimensional simulations of the ozone loss rate with Match observations. In the present study, the transport effects are most important in January 1995 at 500 K and in January and March 2000 at 500 K. They are also visible in the Antarctic at 475 K in the beginning of the winter 2003. It is important to note here that these biases are due to transport effects in the simulation results. They do not necessarily undermine the quality of the experimental Match analysis since the method used to sample the model fields and described in section 3.2 has its own limitations. But the agreement we find here with the results of *Kilbane-Dawe et al.* [2001] indicates that the Match results during January 1995 at that particular level may be biased. The complete evaluation of the Match method has been done elsewhere and is beyond the scope of this paper [e.g., *Morris et al.*, 2005]. In our study, the use of ozone tracers in the simulations allows us to test whether the agreement with the experimental Match results corresponds to effective chemical ozone loss simulated by the model or whether it is fortuitous and due to transport processes within the simulation. Yet, these transport processes may not be correctly modeled and cannot be used directly to evaluate Match trajectories. In our analysis, the use of the 10-day tracer scheme allows us to optimize the estimation of the transport effect since they better represent the passive ozone field for the various Match events all along the winter. Larger tracer changes and unrealistic corrections are generally found using the ozone tracer initialized at the beginning of the simulation.

5.2. Sensitivity of Ozone Loss Rates to the Coupling of ClO and its Dimer and to Total Bromine in the Polar Stratosphere

[29] As mentioned in section 1, recent atmospheric observations have suggested larger levels of bromine compounds

in the Arctic stratosphere and alternative values of kinetic parameters for the coupling of ClO and its dimer. A DOAS measurement of BrO profile [*Fitzenberger*, 2000] over Kiruna, Sweden (68°N), showed a BrO_x (BrO + BrCl) profile [*Canty et al.*, 2005] that is almost the double of the modeled BrO_x values. This extra inorganic bromine is due to the contribution from high level of BrO as measured from DOAS. Standard assumption in the models considers only halons and methylbromide as the source of bromine, which results in up to 16 pptv of total inorganic bromine Br_y. SLIMCAT already accounts for about 6 pptv Br_y from shorter-lived species (as described in section 2.3) yielding about 21–22 pptv of Br_y. This is close to the Br_y derived from the DOAS measurements of BrO, which peaks at about 24 pptv. Current estimates for the contribution from very short lived species (VSLS) range between 3 and 9.4 pptv [*Sinnhuber et al.*, 2002; *Salawitch et al.*, 2005]. All these studies show that total stratospheric Br_y range from 16 pptv (when no VSLS contribution is considered, the old scenario) to the maximum of about 26 pptv (considering maximum contribution from VSLS). Next is the issue of the coupling of ClO and its dimer. Using simultaneous observations of ClO and Cl_2O_2 on board the ER-2 during the THESEO 2000-SOLVE campaign, *Stimpfle et al.* [2004] showed that the dimer photolysis might occur faster than calculated using recommended values of Cl_2O_2 absorption cross-sections. According to this work, the larger values of the rate constant for Cl_2O_2 production given by *Bloss et al.* [2001] and JPL-2002 recommendation are consistent with the observations only if J_{Cl2O2} is calculated with the larger Cl_2O_2 cross sections measured by *Burkholder et al.* [1990]. On the basis of nighttime ClO and Cl_2O_2 measurements, *von Hobe et al.* [2005] suggested relatively smaller values for the ClO/Cl_2O_2 equilibrium constant K_{eq} than the values recommended in JPL-2002. Lower values of K_{eq} result in larger ClO concentrations during the night. This finding is supported by nighttime satellite measurements of ClO [*Berthet et al.*, 2005] and by a recent laboratory measurement by *Plenge et al.* [2005].

[30] To better understand the sensitivity of the model to these various parameters, sensitivity tests were performed with the REPROBUS box model by altering the total bromine values, the Cl_2O_2 photolysis coefficient J_{Cl2O2}, and the ClO/Cl_2O_2 equilibrium constant K_{eq} in the simulation of ozone loss rate. The study focused on the 1999/2000 winter for which the box model simulation underestimated the observed ozone loss rates at 1-sigma standard deviation level in January at 500K. The ozone loss observed in September in Antarctica was also underestimated, particularly at 475 K, but this underestimation was mainly due to the saturation of the loss process caused by the overestimation of the loss rate in the beginning of the winter, as shown in section 4.1. REPROBUS box model test runs were performed for the lower end (16 pptv) and upper end (26 pptv) of total bromine scenarios. For K_{eq}, we used in our test run Fit 3 in the work of *von Hobe et al.* [2005]. Finally, we also tested with the REPROBUS box model the effect of using the J_{Cl2O2} computed with Cl_2O_2 absorption cross-sections from the work of *Burkholder et al.* [1990] (and called Burkholder J_{Cl2O2} hereafter) instead of the JPL-2002 recommended values. It is to be noted that all the REPROBUS box model runs shown in this paper use Burkholder J_{Cl2O2} values with SLIMCAT initialization fields that have already considered some extra bromine amounts (6 pptv) from VSLS.

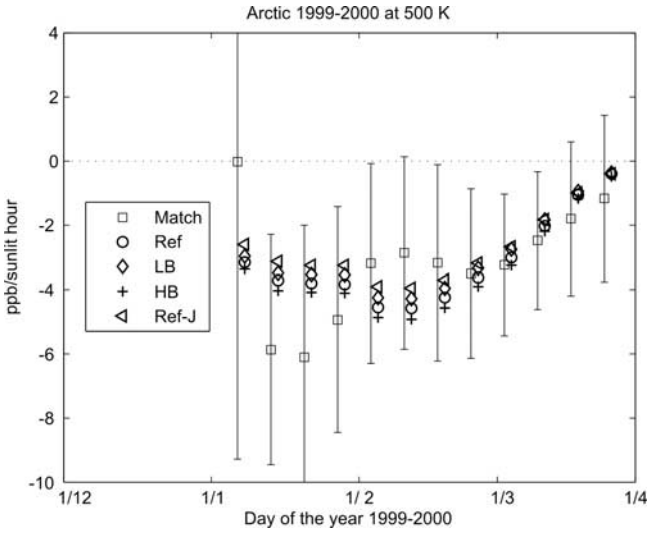

Figure 5. REPROBUS box model simulated ozone loss rates during 1999/2000 at 500 K in different model scenario. Error bars for model runs are not shown for the clarity of figure. 1. Ref: SLIMCAT Bromine and Burkholder J_{Cl2O2}. 2. LB: Lowest Bromine (16 pptv) and Burkholder J_{Cl2O2}. 3. HB: Largest Bromine (26 pptv) and Burkholder J_{Cl2O2}. 4. Ref-J: SLIMCAT Bromine J_{Cl2O2} from JPL-2002 Recommendation. 5. Match: Match results.

[31] The sensitivity tests showed almost no effect of changing K_{eq} on the ozone loss rates (maximum ozone floss rate decreased by 10^{-3} ppbv/sunlit hour), in agreement with results from the work of *von Hobe et al.* [2005]. Hence the tests concentrate on the Cl_2O_2 photodissociation coefficient (for example, computed from JPL-2002 recommendation instead of Burkholder J_{Cl2O2}) and the total bromine content in the simulation. The following four test runs are shown in Figure 5 together with the experimental Match results for the Arctic winter 1999/2000.

[32] 1. Ref: Reference run using SLIMCAT total bromine and Burkholder J_{Cl2O2}.

[33] 2. LB: Lowest total bromine and Burkholder J_{Cl2O2}. For this run, all the bromine component that makes up the total bromine is changed by the ratio $16/Br_y$(total), where Br_y(total) is total bromine from SLIMCAT initialization fields.

[34] 3. HB: The total bromine Br_y is increased to 26 pptv, and Burkholder J_{Cl2O2} is used.

[35] 4. Ref-J: SLIMCAT total bromine, J_{Cl2O2} values from JPL-2002 recommendation.

[36] The error bars for the test runs are not shown for the clarity of the figure. The effect on ozone loss rates of changing the total bromine amount in the simulation from 16 to 26 pptv is largest in January and beginning of February with a maximum change of 0.6 ppbv/sunlit hours or 15% around 12 February. The use of Burkholder J_{Cl2O2} instead of the value recommended by JPL 2002 has a similar effect with a maximum change on ozone loss rate between the simulations (Ref and Ref-J) of 0.3 ppbv/sunlit hour or 7% around the same date. The range of changes in ozone loss rates induced by the sensitivity tests is thus

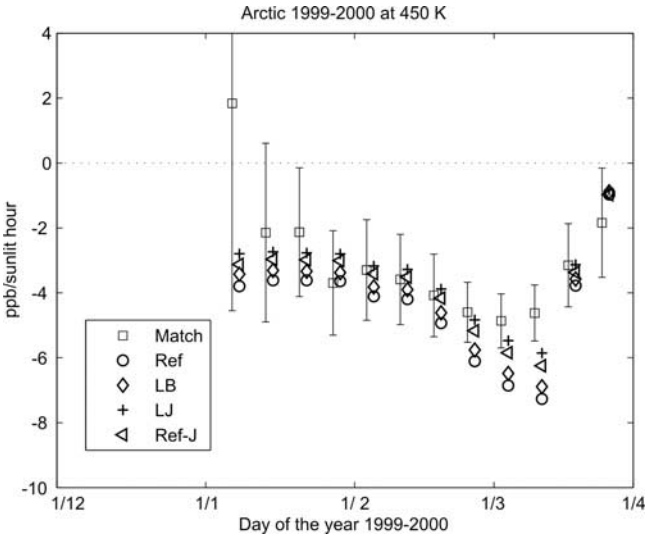

Figure 6. Same as Figure 5 with LB scenario replaced by LJ but at 450 K. 1. Ref: SLIMCAT Bromine and Burkholder J_{Cl2O2}. 2. LB: Lowest Bromine (16 pptv) and Burkholder J_{Cl2O2}. 3. LJ: Lowest Bromine (16 pptv) and J_{Cl2O2} from JPL-2002 Recommendation. 4. Ref-J: SLIMCAT Bromine J_{Cl2O2} from JPL-2002 Recommendation. 5. Match: Match results.

largest during high zenith angle conditions. In the second half of February and March, the effect of changes is smaller because of partial recovery of ClO_x into the $ClONO_2$ reservoir [*Rex et al.*, 1997], as shown in the upper panel of Figure 3. Reduction in ClO amounts affects both the dimer and the ClO + BrO catalytic cycles, which are primarily responsible for the ozone loss in polar regions. The use of Burkholder J_{Cl2O2} and largest total bromine content provides a better agreement of the simulated ozone loss rates with Match observations in January. Yet the largest observed loss rates of 6 ppbv/sunlit hour are still not reproduced by the various test runs, and in February, the simulated ozone loss rates overestimate the observed ones.

[37] We also performed similar sensitivity tests for the level 450 K for which a significant overestimation of the loss rates was obtained with the box model. For these tests, the HB run with largest total bromine content was replaced by a run characterized by the lowest total bromine content and J_{Cl2O2} computed from JPL-2002 recommendation (LJ run). The results are represented in Figure 6. They show that the best agreement with observations is obtained with the LJ scenario that provides the lowest ozone loss rates. Yet, even in this configuration, the box model still overestimates the observed loss rates at 2-sigma level by about 1.2 ppbv/sunlit hour in the beginning of March. Comparable tests were performed for the Antarctic winter 2003 at 475 K where some significant overestimation was also observed in the beginning of the winter (not shown). The tests provide a better agreement with LJ scenario from July to mid-August but at the expense of a larger underestimation at the end of August. Because of the progressive saturation of the loss rates from the end of August, the range between LJ and Ref simulations that provide the lowest and largest loss rates, respectively, decreases from a maximum of 1.2 ppbv/sunlit hour in the beginning of August to near zero in September.

[38] In both series of tests performed in the case of underestimation and overestimation of the ozone loss rates, the maximum difference in ozone loss rates between the various scenarios is on the order of 1.2 ppbv/sunlit hour. This is not sufficient to reach agreement with observed loss rates in the cases where large differences exceeding 2 ppbv/sunlit hour are retrieved. These tests studies have shown that since a reasonable agreement was already achieved with the initial simulations, the various scenarios that tend to increase (or decrease) the ozone loss rate induce a marginal improvement of the retrieved loss rates as compared to the observations. These improvements are made at the expense of a larger overestimation (or a larger underestimation) of the loss rates for other levels and periods of the winters in consideration.

6. Conclusions

[39] Simulations using the three-dimensional MIMOSA-CHIM CTM and a box model using the REPROBUS chemical scheme along Match trajectories and initialized by SLIMCAT fields were performed in order to investigate polar ozone loss rates derived from the Match technique during several recent Antarctic and Arctic winters. Simulated ozone loss rates were generally found to be in reasonably good agreement with the Match results at 2-σ uncertainty level, but the models failed to reproduce at 1-σ the largest ozone loss rates of the order of 6 ppbv/sunlit hour retrieved by the Match technique in the Arctic at 500 K. Yet in some cases, excellent agreement was achieved as for the winter 2002/2003 with both model simulations at 475 K and for the winter 1999/2000 at 450 K with the MIMOSA-CHIM model.

[40] Since larger active chlorine levels are simulated in the box model simulation because of the initial fields provided by SLIMCAT, the ozone loss rates deduced from these simulation are generally larger than those derived from MIMOSA-CHIM simulations. They even exceed the observed ones as in the case of the winter 1999/2000 at the lowermost level and the Antarctic winter 2003 at both levels in the beginning of the winter. Comparison with satellite and in situ ClO measurements indicate that chlorine activation may be overestimated in the box model simulation and SLIMCAT initial fields.

[41] The simulations performed for the Antarctic winter show that saturation effects have to be considered when comparing the modeled and observed loss rates especially if large loss rates are simulated in August. The saturation results in a rapid decrease in ozone loss rates in September. Saturation effects were visible from the end of August in the box model simulation and from mid-September in the Match observations. Saturation was not reached in the three-dimensional simulation during the Match campaign that ended in the beginning of October.

[42] In the case of the three-dimensional simulations, the evaluation of transport effects by computing ozone tracer loss rates shows that in some cases (for example, in the Arctic January 1995 at 500 K and in the Antarctic July 2003 at 475 K), the observed agreement with raw ozone loss rates are accidental and mainly due to tracer loss during the considered Match period. In other cases, the corrected ozone

loss rates show the best agreement as in January 2000 at 500 K. Such dynamical effect seen in the simulations are generally most pronounced at 500 K in the Arctic. In any case, they have to be accounted for when ozone loss rates retrieved by three-dimensional CTM simulations are compared with Match observations.

[43] Test studies with the box model motivated by recent results on the kinetic parameters of the ClO-Cl_2O_2 catalytic cycle and total bromine content in the lower stratosphere resulted in a maximum change in ozone loss rates of 1.2 ppbv/sunlit hour, generally in high solar zenith angle conditions. Simulations with Cl_2O_2 photolysis rates derived from *Burkholder at al.* [1990] measurements, and largest total bromine content of 26 pptv improves the agreement with Match results in some cases but at the expense of an overestimation of the loss rates at the lower levels, taking into account the large active chlorine already simulated by the model. The overall agreement of the model simulations with Match observations shown in this study tends to indicate that the main processes of the chemical ozone loss in both Arctic and Antarctic winters are basically understood. Improvement in box model simulations as compared to previous studies [e.g., *Becker et al.*, 2000] stems mainly from improvements in the SLIMCAT simulation providing the initial fields (for example, a better representation of the subsidence rates and the implementation of a NAT-based denitrification scheme), which results in increased active chlorine levels in the lower polar stratosphere. In this context, the use of stronger Cl_2O_2 photolysis rates and larger total bromine results in a marginal improvement, since large active chlorine levels are already simulated.

[44] The agreement between modeled and observed ozone loss rates found in this study is in general agreement with a recent study by *Frieler et al.* [2006], which concluded that the maximum ozone loss rates retrieved by the Match technique in recent winters were compatible with maximum possible active chlorine level in the lower stratosphere, taking into account recent results on the ClO-Cl_2O_2 cycle and total bromine content. A further detailed assessment of the accuracy of simulated ozone loss rates will require a systematic evaluation of simulated active chlorine levels by independent measurements.

[45] **Acknowledgments.** This work was first supported by the European project QUOBI (Quantitative Understanding of Polar Ozone Loss by Bipolar Investigation) and then by the SCOUT-O3 (Stratospheric-Climate Links with Emphasis on the Upper Troposphere and Lower Stratosphere) European project. We thank the Alfred Wegener Institut for the coordination of ozone soundings and are grateful to the teams in the various sounding stations for providing the ozone measurements. Part of this study is also performed when one of the author (OPT) was in Jet Propulsion Laboratory (NASA) as a National Research Council (NRC) resident research associate. We are also grateful to Stuart McDermid and Thierry Leblanc of JPL Table Mountain Facility for their support in completion of the manuscript. We also thank NILU for providing ECMWF data and an anonymous referee for providing very useful comments on the manuscript.

References

Anderson, J. G., D. W. Toohey, and W. H. Brune (1991), Free radicals within the Antarctic vortex: The role of CFCs in Antarctic ozone loss, *Science*, *251*, 39–46.

Avallone, L. M., and D. W. Toohey (2001), Tests of halogen photochemistry using in situ measurements of ClO and BrO in the lower polar stratosphere, *J. Geophys. Res.*, *106*, 10,411–10,421.

Becker, G., R. Muller, D. S. McKenna, M. Rex, and K. S. Carslaw (1998), Ozone loss rates in the Arctic stratosphere in the winter 1991/92: Model calculations compared with Match results, *Geophys. Res. Lett.*, *25*(23), 4325–4328.

Becker, G., R. Muller, D. S. McKenna, M. Rex, K. S. Karslaw, and H. Oelhaf (2000), Ozone loss rates in the Arctic stratosphere in the winter 1994/1995: Model simulations underestimate results of the Match analysis, *J. Geophys. Res.*, *105*(D12), 15,175–15,184, doi:10.1029/2000JD900056.

Berthet, G., P. Ricaud, F. Lefèvre, E. Le Flochmoën, J. Urban, B. Barret, N. Lautié, E. Dupuy, J. De La Noë, and D. Murtagh (2005), Nighttime chlorine monoxide observations by the Odin satellite and implications for the ClO/Cl_2O_2 equilibrium, *Geophys. Res. Lett.*, *32*(11), L11812, doi:10.1029/2005GL022649.

Bloss, W. J., S. L. Nickolaisen, R. J. Salawitch, R. R. Friedl, and S. P. Sander (2001), Kinetics of the ClO Self-Reaction and 210 nm Absorption Cross Section of the ClO Dimer, *J. Phys. Chem. A*, *105*, 11,226–11,239.

Briegleb, B. (1992), Delta-Eddington approximation for solar radiation in the NCAR community climate model, *J. Geophys. Res.*, *97*(D7), 7603–7612, doi:10.1029/92JD00291.

Brune, W. H., et al. (1991), The potential for ozone depletion in the Arctic polar stratosphere, *Science*, *252*, 1260–1266.

Burkholder, J. B., J. J. Orlando, and C. J. Howard (1990), Ultraviolet absorption cross section of Cl_2O_2 between 210 and 410 nm, *J. Phys. Chem.*, *94*, 687–695.

Canty, T., et al. (2005), Nighttime OClO in the winter Arctic vortex, *J. Geophys. Res.*, *110*(D1), D01301, doi:10.1029/2004JD005035.

Carslaw, K., B. Luo, and T. Peter (1995), An analytic expression for the composition of aqueous HNO_3–H_2SO_4 stratospheric aerosols including gas phase removal of HNO_3, *Geophys. Res. Lett.*, *22*(14), 1877–1880, doi:10.1029/95GL01668.

Chipperfield, M. P. (1999), Multiannual simulations with a three-dimensional chemical transport model, *J. Geophys. Res.*, *104*(D1), 1781–1806, doi:10.1029/98JD02597.

Chipperfield, M. P., M. L. Santee, L. Froidevaux, G. L. Manney, W. G. Read, J. W. Waters, A. E. Roche, and J. M. Russell (1996), Analysis of UARS data in the southern polar vortex in September 1992 using a chemical transport model, *J. Geophys. Res.*, *101*, 18,861–18,881.

Chipperfield, M. P., W. Feng, and M. Rex (2005), Arctic ozone loss and climate sensitivity: Updated three-dimensional model study, *Geophys. Res. Lett.*, *32*, L11813, doi:10.1029/2005GL022674.

Davies, S., et al. (2002), Modeling the effect of denitrification on Arctic ozone depletion during winter 1999/2000, *J. Geophys. Res.*, *107*(D5), 8322, doi:10.1029/2001JD000445, [printed *108*(D5), 2003].

Fahey, D. W., S. Solomon, S. R. Kawa, M. Loewenstein, J. R. Podolske, S. E. Strahan, and K. R. Chan (1990), A diagnostic for denitrification in the winter polar stratosphere, *Nature*, *345*, 698–702.

Feng, W., et al. (2005), Three-dimensional model study of the Arctic ozone loss in 2002/2003 and comparison with 1999/2000 and 2003/2004, *Atmos. Chem. Phys.*, *5*, 139–152.

Fitzenberger, R. (2000), Investigation of the stratospheric inorganic bromine budget for 1996–2000: Balloon borne measurements and model comparison, Differential optical absorption spectroscopy instrument for stratospheric balloon borne trace-gas studies, doctoral dissertation, Univ. of Heidelberg, Heidelberg, Germany.

Frieler, K., M. Rex, R. J. Salawitch, T. Canty, M. Streibel, R. M. Stimpfle, K. Pfeilsticker, M. Dorf, D. K. Weisenstein, and S. Godin-Beekmann (2006), Toward a better quantitative understanding of polar stratospheric ozone loss, *Geophys. Res. Lett.*, *33*(10), L10812, doi:10.1029/2005GL025466.

Glatthor, N., et al. (2004), Spaceborne ClO observations by the Michelson Interferometer for Passive Atmospheric Sounding (MIPAS) before and during the Antarctic major warming in September/October 2002, *J. Geophys. Res.*, *109*, D11307, doi:10.1029/2003JD004440.

Godin, S., V. Bergeret, S. Bekki, C. David, and G. Mégie (2001), Study of the interannual ozone loss and the permeability of the Antarctic polar vortex from aerosol and ozone lidar measurements in Dumont d'Urville (66.4°S, 140°E), *J. Geophys. Res.*, *106*(D1), 1311–1330, doi:10.1029/2000JD900459.

Godin, S., M. Marchand, A. Hauchecorne, and F. Lefèvre (2002), Influence of Arctic polar ozone depletion on lower stratospheric ozone amounts at Haute-Provence Observatory (43.92°N, 5.71°E), *J. Geophys. Res.*, *107*(D20), 8272, doi:10.1029/2001JD000516.

Goutail, F., J.-P. Pommereau, C. Phillips, et al. (1999), Depletion of column ozone in the Arctic during the winters of 1993–94 and 1994–95, *J. Atmos. Chem.*, *32*, 1–34.

Goutail, F., J.-P. Pommereau, F. Lefèvre, M. Van Roozendael, S. B. Andersen, B.-A. Kastad Høiskar, V. Dorokhov, E. Kyrö, M. P. Chipperfield, and W. Feng (2005), Early unusual ozone loss during the Arctic winter 2002/2003 compared to other winters, *Atmos. Chem. Phys*, *5*, 665–677.

Grooβ, J.-U., and R. Müller (2003), The impact of mid-latitude intrusions into the polar vortex on ozone loss estimates, *Atmos. Chem. Phys.*, *3*, 395–402.

Hansen, G., T. Svenoe, M. P. Chipperfield, A. Dahlback, and U.-P. Hopp (1997), Evidence of substantial ozone depletion in winter 1995/96 over Northern Norway, *Geophys. Res. Lett.*, *24*, 799–802.

Hauchecorne, A., S. Godin, M. Marchand, B. Heese, and C. Souprayen (2002), Quantification of the transport of chemical constituents from the polar vortex to midlatitudes in the lower stratosphere using the high-resolution advection model MIMOSA and effective diffusivity, *J. Geophys. Res.*, *107*(D20), 8289, doi:10.1029/2001JD000491.

Heese, B., S. Godin, and A. Hauchecorne (2001), Forecast and simulation of stratospheric ozone filaments: A validation of a high-resolution potential vorticity advection model by airborne ozone lidar measurements in winter 1998/1999, *J. Geophys. Res.*, *106*(D17), 20,011–20,024, doi:10.1029/2000JD900818.

Hoppel, K., R. Bevilacqua, T. Canty, R. Salawitch, and M. Santee (2005), A measurement/model comparison of ozone photochemical loss in the Antarctic ozone hole using Polar Ozone and Aerosol Measurement observations and the Match technique, *J. Geophys. Res.*, *110*, D19304, doi:10.1029/2004JD005651.

Kilbane-Dawe, I., N. R. P. Harris, J. A. Pyle, M. Rex, A. M. Lee, and M. P. Chipperfield (2001), A comparison of Match Ozonesonde-Derived and 3D model ozone loss rates in the Arctic polar vortex during the winters of 1994/95 and 1995/96, *J. Atmos. Chem.*, *39*(2), 123–138.

Lefèvre, F., G. P. Brasseur, I. Folkins, A. K. Smith, and P. Simon (1994), Chemistry of the 1991–1992 stratospheric winter: Three-dimensional model simulations, *J. Geophys. Res.*, *99*(D4), 8183–8195.

Lefèvre, F., F. Figarol, K. S. Carslaw, and T. Peter (1998), The 1997 Arctic ozone depletion quantified from three-dimensional model simulations, *Geophys. Res. Lett.*, *25*, 2425–2428.

Lehmann, R., P. von der Gathen, M. Rex, and M. Streibel (2005), Statistical analysis of the precision of the Match method, *Atmos. Chem. Phys.*, *5*, 2713–2727.

Manney, G. L., and J. L. Sabutis (2000), Development of the polar vortex in the 1999–2000 Arctic winter stratosphere, *Geophys. Res. Lett.*, *27*(17), 2589–2592, doi:10.1029/2000GL011703.

Marchand, M., S. Godin, A. Hauchecorne, F. Lefevre, S. Bekki, and M. Chipperfield (2003), Influence of polar ozone loss on northern mid-latitudes regions estimated by a high-resolution chemistry transport model during winter 1999–2000, *J. Geophys. Res.*, *108*(D5), 8326, doi:10.1029/2001JD000906.

Molina, L. T., and M. J. Molina (1987), Production of Cl_2O_2 from the selfreaction of the ClO radical, *J. Phys. Chem.*, *91*, 433–436.

Morris, G. A., B. R. Bojkov, L. R. Lait, and M. R. Schoeberl (2005), A review of the Match technique as applied to AASE-2/EASOE and SOLVE/THESEO 2000, *Atmos. Chem. Phys.*, *5*, 2571–2592.

Müller, R., et al. (1997), Severe chemical ozone loss in the Arctic during the winter of 1995–1996, *Nature*, *389*, 709–712.

Newman, P., et al. (2002), An overview of the SOLVE/THESEO 2000 campaign, *J. Geophys. Res.*, *107*(D20), 8259, doi:10.1029/2001JD001303.

Plenge, J., et al. (2005), Bond strength of chlorine peroxide, *J. Phys. Chem. A*, doi:10.1021/jp044142h.

Proffitt, M. H., et al. (1990), Ozone loss in the Arctic polar vortex inferred from high altitude aircraft measurements, *Nature*, *347*, 31–36.

Proffitt, M. H., K. Aikin, J. J. Margitan, M. Loewenstein, J. R. Podolske, A. Weaver, K. R. Chan, H. Fast, and J. W. Elkins (1993), Ozone loss inside the northern polar vortex during the 1991–92 winter, *Science*, *261*, 1150–1154.

Rex, M., et al. (1997), Prolonged stratospheric ozone loss in the 1995–96 Arctic winter, *Nature*, *389*, 835–838.

Rex, M., et al. (1999), Chemical ozone loss in the Arctic winter 1994/1995 as determined by the Match technique, *J. Atmos. Chem.*, *32*, 1–34.

Rex, M., et al. (2002), Chemical depletion of Arctic ozone in winter 1999/2000, *J. Geophys. Res.*, *107*(D20), 8276, doi:10.1029/2001JD000533.

Rex, M., R. J. Salawitch, M. L. Santee, et al. (2003), On the unexplained stratospheric ozone losses during cold Arctic Januaries, *Geophys. Res. Lett.*, *30*(1), 1008, doi:10.1029/2002GL016008.

Ricaud, P., et al. (2005), Polar vortex evolution during the 2002 Antarctic major warming as observed by the Odin satellite, *J. Geophys. Res.*, *110*, D05302, doi:10.1029/2004JD005018.

Salawitch, R., et al. (1990), Loss of ozone in the Arctic vortex for the winter of 1989, *Geophys. Res. Lett.*, *17*(4), 561–564, doi:10.1029/90GL00184.

Salawitch, R. J., et al. (1993), Chemical loss of ozone in the Arctic polar vortex in the winter of 1991–1992, *Science*, *261*, 1146–1149.

Salawitch, R. J., D. K. Weisenstein, L. J. Kovalenko, C. E. Sioris, P. O. Wennberg, K. Chance, M. K. W. Ko, and C. A. McLinden (2005), Sensitivity of ozone to bromine in the lower stratosphere, *Geophys. Res. Lett.*, *32*, L05811, doi:10.1029/2004GL021504.

Sander, S. P., et al. (2003), Chemical kinetics and photochemical data for use in stratospheric modeling, *Evaluation 14*, JPL Publ., p. 02–25.

Santee, M. L., G. L. Manney, N. J. Livesey, L. Froidevaux, I. A. MacKenzie, H. C. Pumphrey, W. G. Read, M. J. Schwartz, J. W. Waters, and R. S. Harwood (2005), Polar processing and development of the 2004 Antarctic ozone hole: First results from MLS on Aura, *Geophys. Res. Lett.*, *32*, L12817, doi:10.1029/2005GL022582.

Shine, K. P. (1987), The middle atmosphere in the absence of dynamical heat fluxes, *Q. J. R. Meteorol. Soc.*, *113*, 603–633.

Sinnhuber, B.-M., et al. (2002), Comparison of measurements and model calculations of stratospheric bromine monoxide, *J. Geophys. Res.*, *107*(D19), 4398, doi:10.1029/2001JD000940.

Solomon, S. (1999), Stratospheric ozone depletion: A review of concept and history, *Rev. Geophys.*, *37*(3), 275–316.

Stimpfle, R. M., D. M. Wilmouth, R. J. Salawitch, and J. G. Anderson (2004), First measurements of ClOOCl in the stratosphere: The coupling of ClOOCl and ClO in the Arctic polar vortex, *J. Geophys. Res.*, *109*, D03301, doi:10.1029/2003JD003811.

Streibel, M., et al. (2006), Chemical ozone loss in the Arctic winter 2002/2003 determined with Match, *Atmos. Chem. Phys.*, *6*, 2783–2792.

Tripathi, O. P., et al. (2006), High resolution simulation of recent Arctic and Antarctic stratospheric chemical ozone loss compared to observations, *J. Atmos. Chem.*, *55*, 205–226, doi:10.1007/s10874-006-9028-8.

Vogel, B., W. Feng, M. Streibel, and R. Müller (2006), The potential impact of ClOx radical complexes on polar stratospheric ozone loss processes, *Atmos. Chem. Phys.*, *6*, 3099–3144.

Vömel, H., D. W. Toohey, T. Deshler, and C. Kroger (2001), Sunset observations of ClO in the Arctic polar vortex and implications for ozone loss, *Geophys. Res. Lett.*, *28*, 4183–4186.

von der Gathen, P., et al. (1995), Observational evidence for chemical ozone depletion over the Arctic in winter 1991–92, *Nature*, *375*, 131–134.

von Hobe, M., et al. (2005), A re-evaluation of the ClO/Cl_2O_2 equilibrium constant based on stratospheric in situ observations, *Atmos. Chem. Phys.*, *5*, 693–702.

von Hobe, M., et al. (2006), Understanding the kinetic of the ClO-dimer cycle, *Atmos. Chem. Phys. Discuss.*, *6*, 7905–7944.

Wamsley, P. R., et al. (1998), Distribution of halon-1211 in the upper troposphere and lower stratosphere and the 1994 total bromine budget, *J. Geophys. Res.*, *103*, 1513–1526.

World Meteorological Organization (WMO) (1992), Scientific assessment of ozone depletion: 1991, in *Global Ozone Research and Monitoring Project, WMO Rep 25*, Geneva, Switzerland.

World Meteorological Organization (WMO) (2003), Scientific assessment of ozone depletion: 2002, *Report No. 47*, Geneva, Switzerland.

Woyke, T., R. Muller, F. Stroch, D. S. McKenna, A. Engel, J. J. Margitan, M. Rex, and K. S. Karslaw (1999), A test of our understanding of the ozone chemistry in the Arctic polar vortex based on in-situ measurements of ClO, BrO, and O_3 in the 1994/1995 winter, *J. Geophys. Res.*, *104*(D15), 18,755–18,768.

M. Chipperfield and W. Feng, Institute for Atmospheric Science, University of Leeds, Leeds, LS2 9JT, United Kingdom.

S. Godin-Beekmann, A. Hauchecorne, F. Lefèvre, and A. Pazmiño, Service d'Aéronomie–IPSL du CNRS, Université Pierre et Marie Curie, Paris 75252, Cedex 05, France.

G. Millard, Department of Earth Sciences, University of Cambridge, Cambridge, CB2 3EQ, United Kingdom.

M. Rex, M. Streibel, and P. von der Gathen, Alfred Wegener Institute for Polar and Marine Research, Telegrafenberg A43, Potsdam, D-14473, Germany.

O. P. Tripathi, NASA–Jet Propulsion Laboratory, California Institute of Technology, Table Mountain Facility, 24490 Table Mountain Road, Wrightword, CA 92397, USA. (ompraka@aero.jussieu.fr; tripathi@tmf.jpl.nasa.gov)